Constant-Q Graphic Equalizers*

DENNIS A. BOHN

Rane Corporation, Mountlake Terrace, WA 98043, USA

A new class of graphic equalizers is presented that is characterized by being constant-Q and shown to offer significant advantages over conventional RLC and gyrator based designs. Only constant-Q designs are, in fact, true "graphic" equalizers. Included is an introductory tutorial on the design requirements and trade-offs of constant-Q circuitry, as well as a discussion regarding the combining characteristics of each class of equalizer. Shown is that all equalizers combine equally for the same bandwidths. Finally, areas requiring future research are outlined and discussed.

0 INTRODUCTION

The constant-Q one-third octave graphic equalizer revolution is under way. Its roots go back to the mid-1970s, but real progress and advancement did not occur until 1981.

The year 1976 saw the development of a new topology for 10-band octave equalizers [1], featuring minimum phase, very smooth combining characteristics, and an almost total lack of adjacent band interference. This offered an alternative to the inductor and gyrator designs of that time. It was not, however, constant-Q. Further, restrictions to low values of Q made one-third-octave applications impossible.

In 1981, Greiner and Schoessow [2] did an extensive analysis of this circuit (and others), proving it to be minimum phase and demonstrating its lack of adjacent band interference. In this same paper they showed a variation of the circuit that *was* constant-Q, but it suffered from interactive adjacent bands and asymmetrical boost/cut performance.

While researching this paper, three true constant-Q one-third-octave graphic equalizers emerged. All were concurrently designed in 1981 [3]-[5]. (This is another example of the many interesting instances of independently simultaneous developments in technology.) Since that time, other constant-Q designs have reached the marketplace. The past years have produced enough confusion regarding constant-Q versus nonconstant-Q

designs to warrant a permanent record of their origin and to classify their characteristics. This paper will undertake both in an objective and scientific manner.

1 BACKGROUND

The author came to the decision that a constant-Q design was necessary after designing a one-third-octave graphic equalizer based on current (1981) practices. Two things were learned: the designs were not constant-Q; and they were not acceptable for graphic equalizer applications. The problem was that the bandwidth degraded drastically at all but full boost/cut positions. This made completely false the idea that the front panel settings provided a "graphical" representation. The settings at modest boost/cut positions did not even resemble the actual curve response. It became obvious that the only way to achieve truly "graphical" performance was to derive a constant-Q design.

Having designed several parametric equalizers characterized by totally independent control of amplitude prior to this project (dating back to 1977), clearly a similar topology was needed. The development of the constant-Q graphic equalizer followed immediately from this realization and implementation.

Independently Snow [4] came to design his company's first one-third-octave equalizer. Recognizing the limitations of the commonplace practices of the time and drawing on his parametric design background (also dating back to 1977), he designed a true state-variable filter approach. This solution achieved minimal adjacent channel interaction, constant bandwidth, and very low component sensitivities.

In the same time frame, and also independently, Nova [5] designed a one-third-octave graphic equalizer for his company. Not satisfied with gyrator performance, he developed a strikingly similar variation of the parametric approach used by this author and Snow (all without collaboration). Unique was his use of three summing circuits executed with only four operational amplifiers.

All of these products were introduced to the public in 1982. This marks the official birth of the commercially available constant-Q one-third-octave graphic equalizer.

2 CONSTANT-Q VERSUS CONVENTIONAL GRAPHIC EQUALIZERS

Sadly, most modem graphic equalizers represent a poor application of new technology. What transpired was taking the old passive RLC circuits and updating them into an active counterpart, using gyrators [6] instead of inductors. Had there been no shortcomings with the old designs, this would not be such a negative aspect. Nevertheless, there was a serious shortcoming—the bandwidth changed for every slider position. It was only narrow at the maximum boost or cut points. At all other slider positions it became wider and wider. This makes a mockery out of the name "graphic" equalizer. The front panel settings have nothing to do with the actual frequency response [7].

Simply building a gyrator equalizer that mimicks classic passive types does not make for a more useful or better device. In fact, this approach can be wastefully constrictive. A truly effective use of gyrators involves redefining the overall function, rather than simply implementing classic equalizers in a different way. (For a detailed discussion of a typical gyrator graphic equalizer, see [8]; for a circuit critique of the bandwidth problems associated with RLC and gyrator graphic equalizers, see [2], [9].)

Pennington [10] has done extensive computer simulation studies of the differences between constant-Q and RLC/gyrator designs. Figs. l-6 are reproduced here with permission from the publisher of his work.

These figures compare the results from a one-third-octave constant-Q graphic equalizer design (left) with those of a one-third-octave conventional design (right). In all figures the sliders were set, to identical positions between the units, and the input drive signal was held constant. Each represents a sine-wave swept spectrum analysis result for different slider positions.

Fig. l(a) shows the results for the constant-Q design with one slider set to +3 dB; Fig. 1(b) shows the comparable results for the conventional example. Note the bandwidth comparison between the two. The conventional design's bandwidth is in excess of one octave. It is no longer functioning as a one-third-octave equalizer; it has degraded into something nearer to a 10-band octave equalizer.

Fig. 2(a) is the above case with the slider moved to the +6 dB position. Note that the bandwidth is the same as in Fig. l(a), the only change being the peak amplitude. Compare this with the results in Fig. 2(b) for the conventional design. The bandwidth has decreased from what it was in Fig. l(b), but it still has not approached one-third of an octave—and will not until the slider position reaches maximum.

Fig. 3(a) shows the contant-Q equalizer with three adjacent sliders set to +3 dB, –3 dB, and +3 dB, respectively. As can be seen, the amplitude does not fully reach either +3 dB or –3 dB. However, all three of the controls yield approximately the expected results: an increase, a decrease, and an increase in amplitude. Fig. 3(b) is the conventional equalizer again, and the ineffectiveness of its controls becomes quite evident. The settings are the same as on the equalizer in Fig. 3(a); however, there is a noticeable lack of effect present on the center filter. Its only effect is to reduce the peak amplitude of its neighbors. This is obviously in contradistinction to what the front panel controls show.

Fig. 4(a) shows the result of setting three adjacent filters to +6 dB, +0 dB, and +6 dB on a constant bandwidth equalizer, All three controls exhibit the expected effect. Fig. 4(b) demonstrates the imprecision of the conventional equalizer under the same conditions. Not only is there no attempt to return to zero, but the total effect is a peak amplitude of almost 9 dB. Comparison is impossible between the front panel settings and the results.

Fig. 5(a) is a sweep of the constant-Q graphic with two adjacent controls set to +3 dB and +6 dB. The discrete effect, that the two filters have on the passband is evident. Fig. 5(b) shows the conventional equalizer under the same conditions. No step is observed, only a combined peak 8 dB high and nearly one octave wide.

Fig. 6(a) illuminates the one visually displeasing aspect of the constant-Q equalizer; however, this effect is of no audible consequence. (Much more on the combining characteristics of graphic equalizers later.) It is the author's opinion that setting three adjacent controls to +6 dB must (if it is a true one-third-octave graphic equalizer) yield a +6 dB reponse over exactly one octave (three one-thirds), rather than the off-scale, 2.5-octave-wide response depicted in Fig. 6(b) under the same conditions. (It went to +12.5 dB at-its peak.)

These figures show that there is a distinct difference between the two designs. Choose a constant-Q, true one-third-octave graphic equalizer, which gives the expected results as indicated on the front panel, or a conventional design whose bandwidth varies to such great extremes, that-there is no way of knowing what the relationship is between the controls of the device and the frequency response of the audio passing through it.
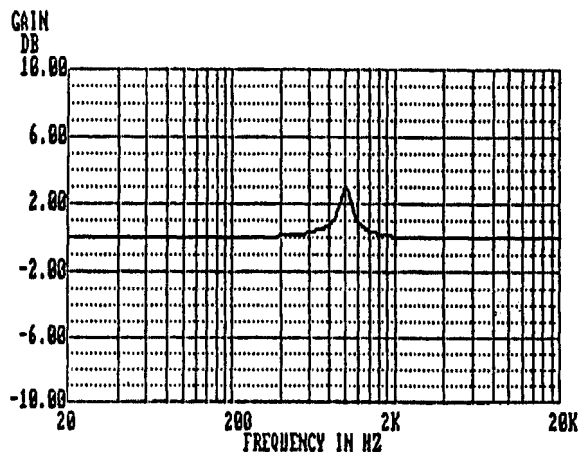
3 CONSTANT-Q CIRCUITRY

Several possible methods of obtaining constant-Q performance follow, with the hope of stimulating other designers to discover even better approaches. There is only one rule: *The amplitude function must be entirely separate from the bandpass filter function.*
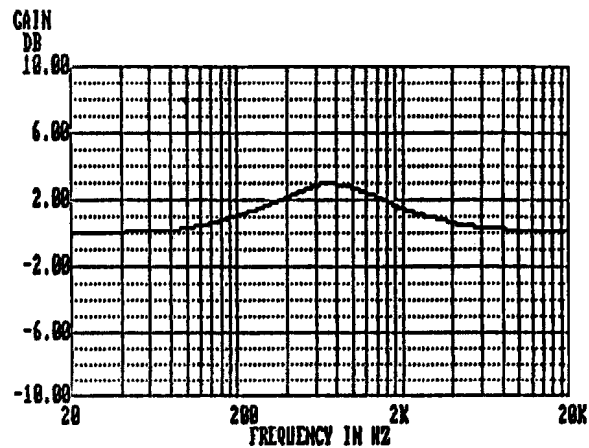
3.1 Case 1—Symmetrical Boost/Cut Topology

Drawing from personal parametric design experience, the easiest approach seemed to be to adapt proven parametric topology to graphic equalizer functions. Fig. 7 shows a typical approach to parametric design. The earliest reference found for this configuration is from Gundry [11], but there may be still others that predate it. The beauty of this approach lies in its utter simplicity. Any number of state-variable filter sections can be paralleled between two inverting summing amplifiers. The slider serves to route the output of each filter section either to the first summer for cutting or to the second summer for boosting, with the grounded center tap guaranteeing flat response in the center detent position.

(a)

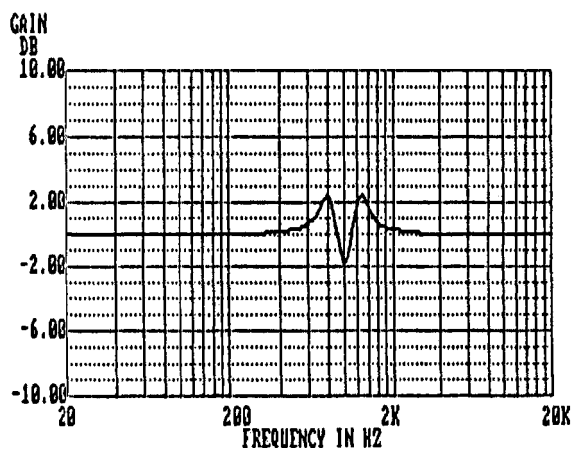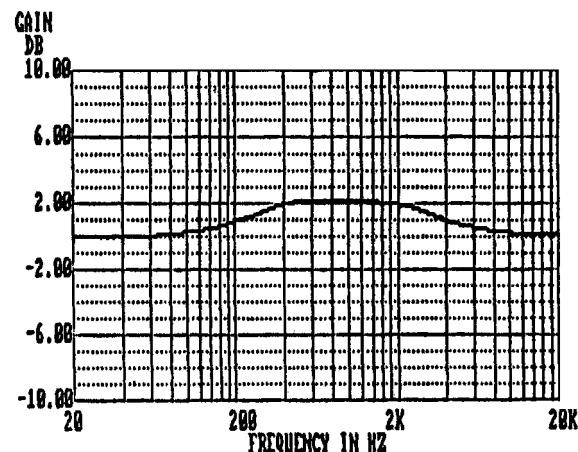
(b)

Fig. 1. One slider set to +3 dB.

(a)

(b)

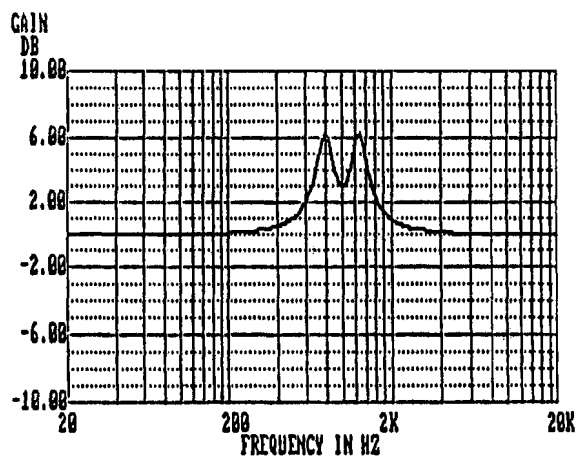Fig. 2. One slider set to +6 dB.

(a)

(b)

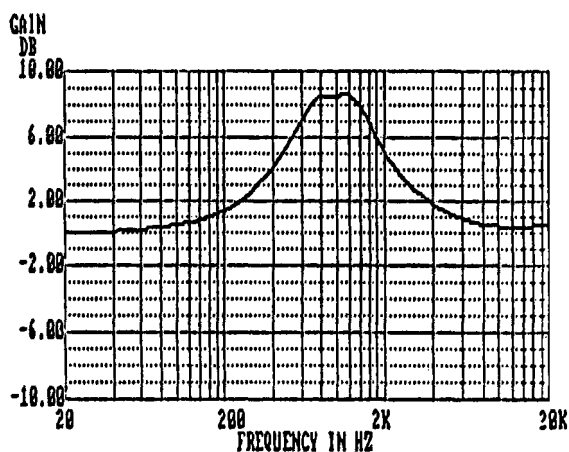Fig. 3. Three adjacent sliders set to +3 dB, -3 dB, and +3 dB.

Boosting is accomplished by summing the bandpass (BP) output of the state-variable filter with the original signal. By weighting the series output resistor of the filter network *R2,* any amount of boost can be achieved. Symbolically the output becomes $1 + k$ BP, where 1 represents the normalized full frequency input and k the scaling factor. For example, +12 dB (x4) boost

would require $k = 3$. The result would be 1 times the original signal plus 3 times the filter function, yielding 4 times those signals at the filter center frequency, or +12 dB boost.

Cutting is simply the inverse of boosting. This is done with the first summer by reconfiguring the BP filter to the feedback loop (accomplished by positioning
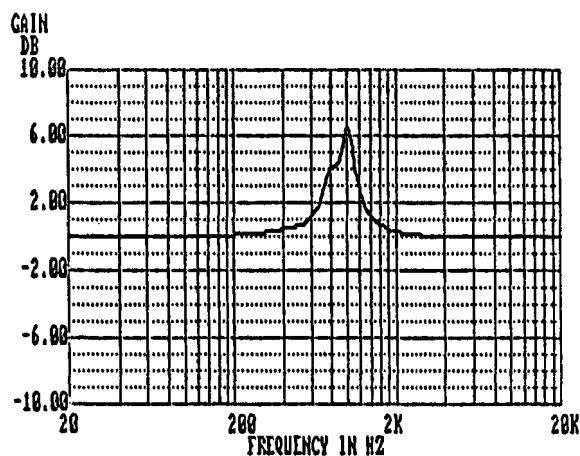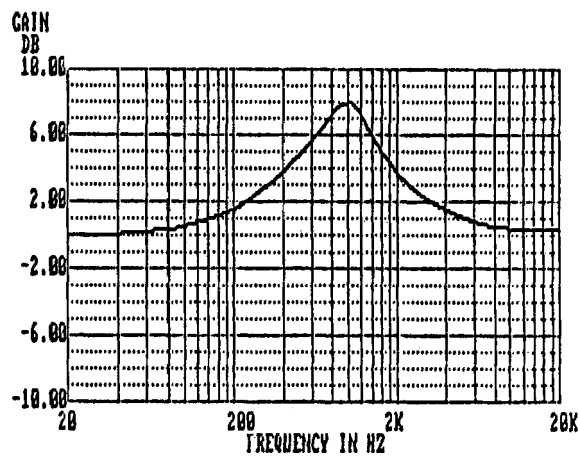

Fig. 4. Three adjacent sliders set to +6 dB, 0 dB, and +6 dB.

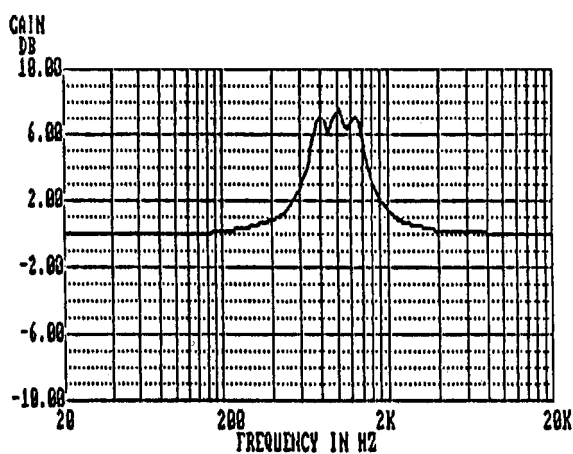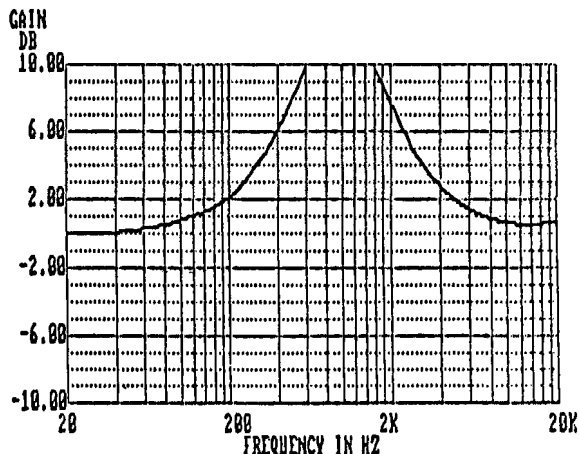Fig. 5. Two adjacent sliders set to +3 dB and +6 dB.

Fig. 6. Three adjacent sliders set to +6 dB.

the slider to the extreme left). The output of the first summer is now $l/(1+ k$ BP). (This results in reciprocalcurves for both boost and cut, which are usually the preferred choice.) The input and feedback resistors of the first summer are the same as for the second summer for equal values of boost and cut. For different values of cut, resistors R3 are changed accordingly but kept equal to each other to maintain unity gain times the input signal. For the above example, the output level at the filter center frequency now becomes ¼, or –12 dB.

For graphic equalizer applications, the center frequency and bandwidth requirements are fixed. Fig. 7 can then be redrawn as Fig. 8 to produce a constant-Q design. This satisfies the rule that the amplitude function must be independent from the filter function. Each bandpass filter section is a separate entity, with all boosting and cutting being done by the two summers. The reciprocal results appear in Fig. 9. (A detailed discussion of case 1 regarding BP filter requirements and multiple summers is given in Section 4.)

3.2 Case 2—Asymmetrical Boost/Cut Topology

Constant-Q graphic equalizer designs requiring asymmetrical boost/cut performance can be achieved with the circuit shown in Fig. 10. The boost function is similar to that of Fig. 8 except for a weighted differencing network on the output.

Cutting is now a subtractive process rather than an inverse process as before. Essentially the net result is $1 + k$ BP for boost and $1 - k$ BP for cut. Specifically for the ±12 dB example shown, the cut output is 1.25BP – 1, yielding a gain of ¼ at the filter center frequency, or –12 dB cut. Results for a l kHz section appear in Fig. 11.
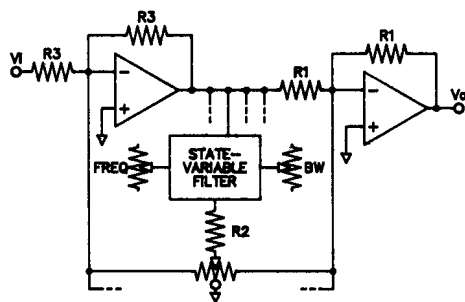
Fig. 12 shows an alternate asymmetrical constant-Q topology due to Van Ryswyk [12], [13]. The output of the BP filter is added to the original signal for boosting and subtracted for cutting. The position of the slider dictates how much of either is delivered to the final output. (The grounded center tap has been added by the author.) Fig. 11 applies equally well to Fig. 12.

The circuit shown in Fig. 12 provides only one frequency band per section, as compared with all previous circuits where any number of BP sections could be paralleled between the two summers. This is a serious drawback.

3.3 Case 3—Transveral Constant-Q Topology

The first commercially available graphic equalizer (15 bands) employing transversal filters was introduced by Industrial Research Products, Inc. [14] in 1984. This marks a new category of constant-Q graphic equalizers.

Transversal filters are a unique breed, requiring no capacitors or inductors to synthesize the equalizer response. They rely, instead, on time delay blocks and weighted summing. It is beyond the scope of this paper to present a detailed account of transversal filter design theory. Interested readers should consult the many books on this subject, [15] being an excellent source. An introduction, however, is possible.

A typical transversal filter graphic equalizer-block diagram appears in Fig 13. A tapped delay line forms the heart of the transversal filter. Each tap roughly represents an area of the frequency response affected. By scaling each of these outputs by a "tap weight" (constants a_1, a_2, etc.) and then summing the results, any desired frequency response can be obtained.

The tapped delay line may be implemented with an analog delay line (normally using analog bucket-brigade devices) or digital shift registers. This is the distinction between analog and digital transversal filters. The term "transversal filter" does not mean "digital filter"; it is the entire family of filter functions done by means of

Fig. 7. Parametric equalizer topology.

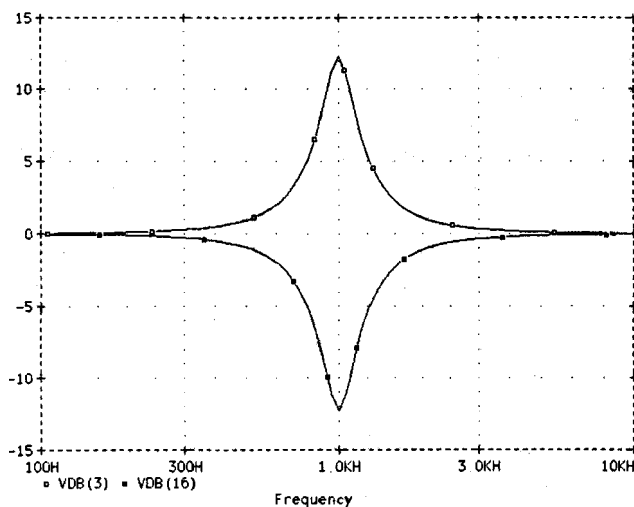Fig. 8. Case l—symmetrical constant-Q graphic equalizer topology.

Fig. 9. Symmetrical boost/cut performance, case 1.

a tapped delay line. There exists a class of digital filters realized as transversal filters, using a shift register rather than an analog delay line, the inputs being numbers rather than analog functions. To date, however, due to very expensive hardware, digital transversal filter realization of a true one-third-octave graphic equalizer remains in the laboratory.

Transversal filters offer many advantages for graphic equalizer designs. Linear phase shift is the principal advantage. Due to the lack of energy storage elements within the filter (inductors or capacitors), there is always linear phase shift, that is, pure time delay independent of frequency. This results in no group delay distortion, guaranteeing perfect transient response.

Other advantages include minimum adjacent band interaction and very little combined ripple. As always, though, there is a price. The price today is either dollars (digital transversal filters) or performance (analog transversal filters).

Several annoying shortcomings plague analog bucket-brigade devices. Their lack of dynamic range, and high noise levels necessitate companding tricks for acceptable levels of performance. This results in increased cost

to constant-Q graphic design. The operational amplifier and passive partscount is almost identical to its gyrator counterpart, allowing a design that is just as cost effective and reliable; but with superior performance. The simplicity and elegance of the boost/cut circuits, along with their simple design rules, make case 1 easy to implement. Manufacturing repeatability is assured since all critical specifications are set by resistors and capacitors, which can be bought to whatever precision is required. Using precision passive parts allows the design of a complete one-third-octave equalizer without any trim pots. This makes production time short and field reliability high.

Case 1 achieves symmetrical boost/cut performance about a true 0 dB reference line while maintaining constant bandwidth at all slider positions. Use of grounded center-tapped sliders guarantees that each filter section is completely removed from the signal path when not needed, and that neighboring band interference is minimized.

Using the analysis techniques of Greiner and Schoessow [2], it can be shown that case 1 exhibits minimum phase behavior for all combinations of control settings,
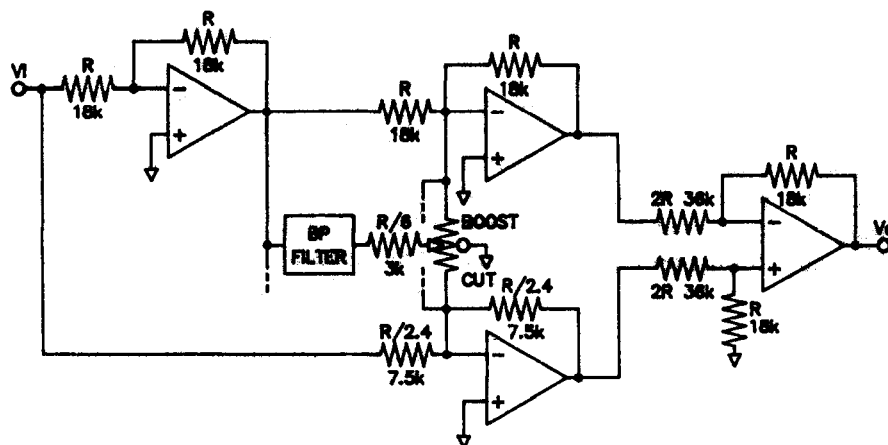

Fig. 10. Case 2—asymmetrical constant-Q graphic equalizer topology.

and complexity, along with the problems of accurate tracking. Careful trimming is required using specialized circuits if the distortion levels are to be reduced to professional levels.

The last area requiring attention when applying transversal filters to graphic equalizers is the development of real boost/cut topologies exhibiting symmetrical responses. Boost/cut functions should be referenced to 0 dB, neither cutting from a maximum gain position nor boosting from an attenuated starting point. Reciprocal (symmetrical) boost/cut curves are universally preferred by sound installers.

These problems will be solved. They have to be; the technology is too exciting to lie dormant.

4 OPTIMIZING CASE 1

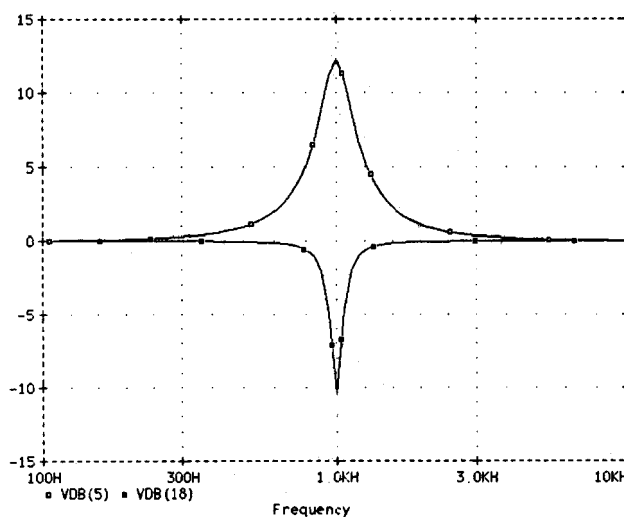Case 1 seems to represent the best overall approach

Fig. 11. Asymmetrical boost/cut performance, case 2.

that is, the transfer functions have no zeros in the right-half s plane. The circuit is also unconditionally stable since all poles lie in the left-half s plane. Mathematically speaking, case 1 has only positive real transfer functions. (As an editorial aside, this whole issue of minimum phase represents an example of how marketing personnel abuse technical phrases. Various manufacturers flaunt the term "minimum phase" as if they invented it, implying that the competition is not minimum phase. In fact, no examples of commercially available graphic equalizers exist that are *not* minimum phase.)

For these reasons, case 1 is selected for optimizing. Several things need to be analyzed for optimization. First, the order of the bandpass filter needs to be determined. Next, the best topology which provides that order must be selected. Then the best way to recombine the filter outputs for minimum ripple content must be thought out. Finally, the noise behavior of the circuit has to be minimized.

4.1 Bandpass Filter Order

For simplicity of analysis and discussion, Fig. 8 is redrawn as a "half-circuit" in Fig. 14. Just the boost mode is represented, showing two bandpass filter sections with their sliders positioned at maximum. In this position the slider control itself drops out of the circuit, since one side is at virtual ground and the other side

(center tap) is at actual ground. This circuit allows analysis of two adjacent bands summed together at full boost.

Determination of the optimum filter order is worth an investigation. Costs usually dictate that commercial one-third-octave graphics will consist of second-order bandpass filter sections, but are they the best choice from a performance standpoint?

Ideally, the bandpass filter would possess the perfect brickwall response shown dashed in Fig. 15. It would be exactly one-third-octave wide, geometrically symmetric about the center frequency f_0, and it would have no phase shift. So much for idealism.

A two-pole and four-pole realizable approximation to the ideal is shown by the solid lines with open and solid square legends, respectively. There are two cutoff points (shown as f_1 and f_2) that occur by definition where the magnitude decreases 3 dB from its maximum value. For the realizable approximation, the bandwidth is then $f_1 - f_2$. Since the center frequency is the geometric mean of frequencies f_1 and f_2, they will be located one-sixth octave on either side of f_0 for the one-third-octave bandwidth case.

Butterworth responses are shown, but Chebyshev could be used. The Chebyshev approximation to an ideal filter has a much more rectangular response in the region near cutoff than has the Butterworth family.
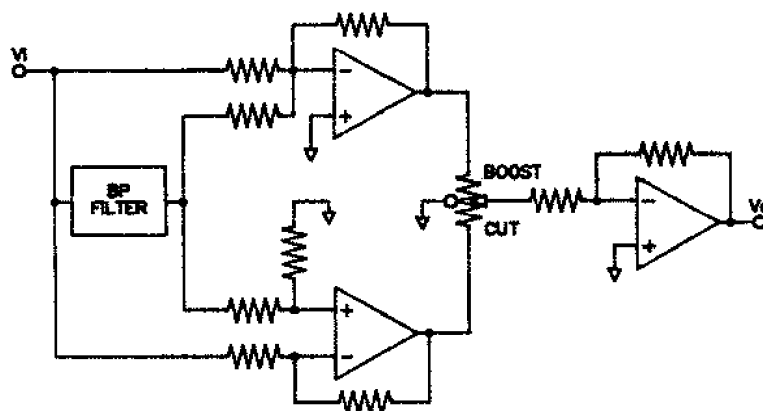

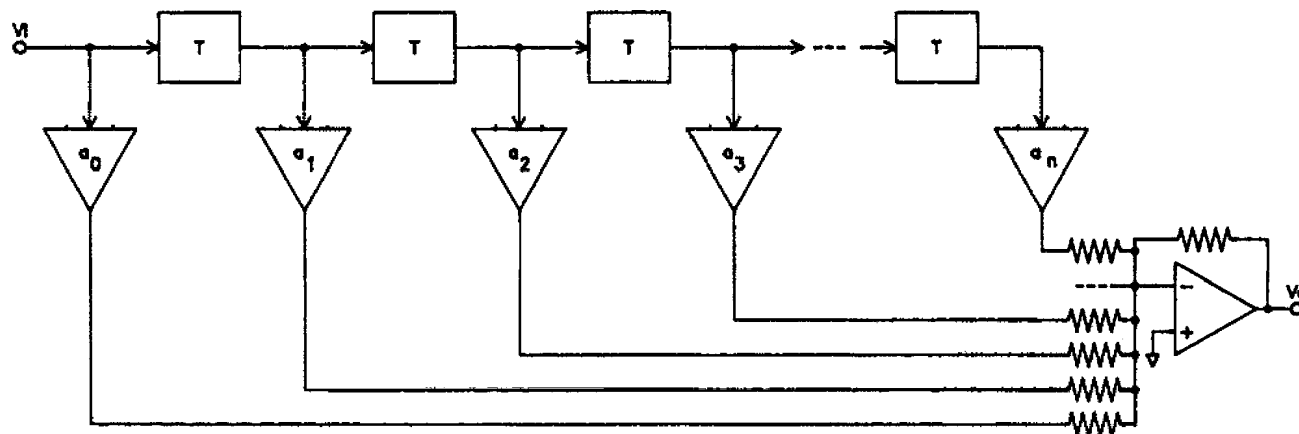Fig. 12. Alternate asymmetrical constant-Q topology.

Fig. 13. Transversal filter graphic equalizer.

This is accomplished, however, at the expense of allowing ripples in the passband with an associated increase in phase shift. Butterworth has monotonic amplitude response with a maximally flat passband, less phase shift, and better transient results; in conclusion, it is the preferred choice.

The required Q for these approximations can be found directly from the closed solution given in [16]. In addition, given any Q, the reverse—the bandwidth in octaves—can be calculated. (This is not as obvious as it may seem and will be useful in the discussion on combining later.) Using this formula, Q is calculated to be 4.318.

Examination of Fig. 15 suggests that the four-pole approximation is preferred since it comes closer to the ideal shape. Further investigation, however, will reveal this not to be the case.

Of interest is how well two adjacent bands will add together. Figs. 16 and 17 show the response of two adjacent two-pole and four-pole filter sections, respectively. Fig. 18 shows the two-pole summed result superimposed over the individual curves, and Fig. 19 shows the summed curve for the four-pole case (the individual responses were omitted for clarity). Fig. 18 is encouraging, but Fig. 19 is not. The middle is cancelling; not something to be expected from a casual inspection of Fig. 17. To understand Fig. 19, the phase responses of Fig. 15 must be examined.

Fig. 20 shows the associated phase shift characteristics of the curves displayed in Fig. 15. Here it is seen that in the two-pole case the phase shift at the crossover point (one-sixth octave away from each f_0) will be ±45 deg, but it increases to ±66 deg in the four-pole example. The magnitudes in all cases will be 0.707 (–3 dB). Fig. 21 diagrams the vector arithmetic for the sums of each. *The two-pole case represents the ideal by summing to unity with 0 deg phase shift.* The four-pole case also yields 0 deg phase shift, but the magnitude drops to –4.8 dB. It remains to be seen how well each will perform in the test circuit of Fig. 14.

Running the circuit in Fig. 14 with two-pole filters produces the results shown in Fig. 22. Everything is well-behaved and as expected. Note that the crossover point magnitude is exactly 12 dB, demonstrating that the skirts canceled as shown in Fig. 21. The "horns" are due to the skirt overlap between adjacent bands. At the exact center frequency of each, the neighbor's contribution is –7 dB at 116 deg, resulting in a combined response 1 dB higher than desired. It should also be observed that the ripple is less than in Fig. 18,
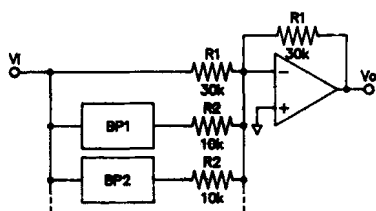
where just the two filters were summed. By adding this result with the original signals, as done in Fig. 14, the skirt effect is diluted.

Running the same circuit with four-pole filters results in Fig. 23. The middle point reduction is still observed
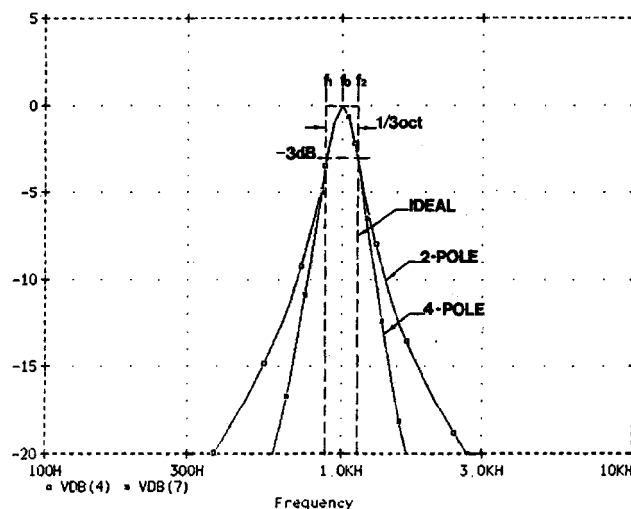

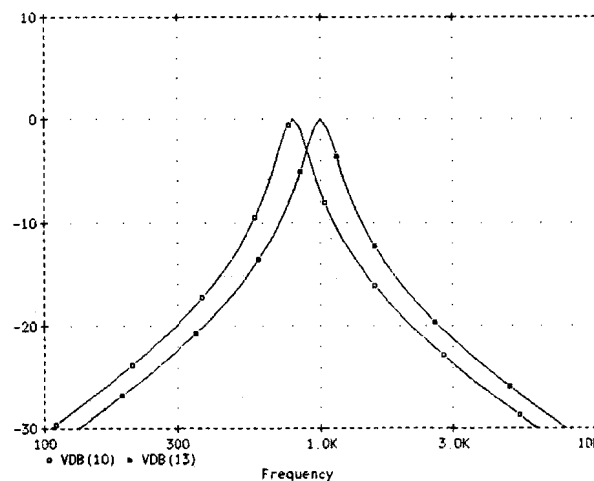Fig. 15. Ideal two-pole and four-pole bandpass responses.
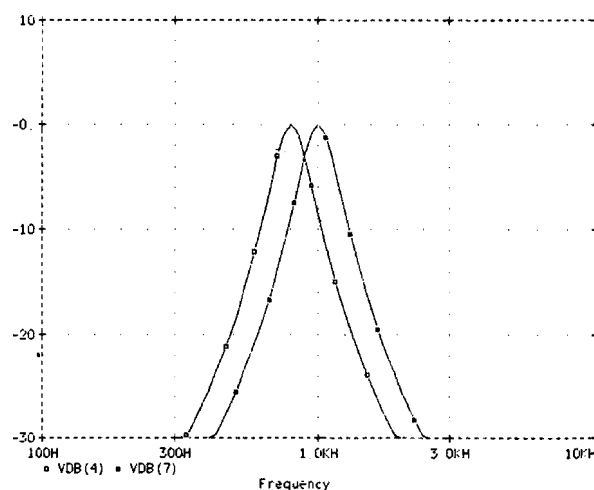

Fig. 16. Adjacent two-pole filters.

Fig. 17. Adjacent four-pole filters.

Fig. 14. Full boost "half-circuit" for +12 dB.

along with a new problem: the out-of-band frequencies are experiencing reduction due to the excessive phase shift of the four-pole filters. What is going on is that at the center frequency of each filter the signals are in phase, 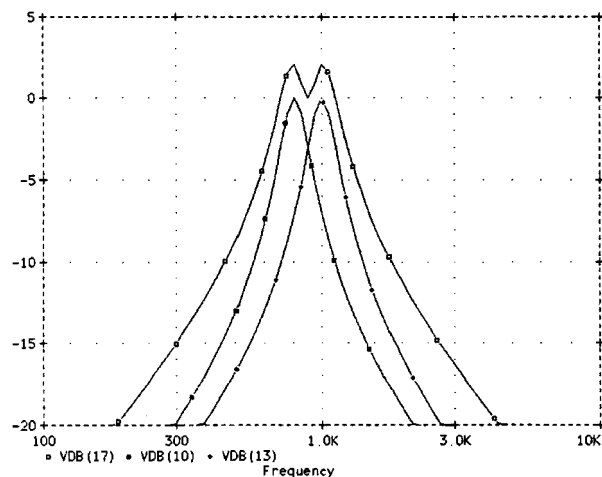but at the extremes the phase shift is approaching 180 deg with respect to the original. Adding these together produces reduced magnitudes. This suggests that inverting the main signal before summing with the filter outputs may produce interesting results. It does.

Fig. 24 shows the effect. The inverter does fix the side lobes but produces disastrous results at the crossover point. A 10 dB-deep hole is not encouraging. In short, *the four-pole approach will never sum properly with its adjacent neighbors.* Since all higher order filters only get worse, two-pole is the optimum order of choice.

Fig. 18. Summed response of adjacent two-pole filters.
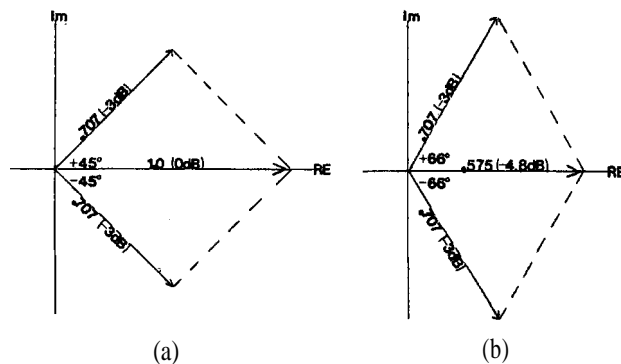

(a)   (b)

Fig. 21. Vector arithmetic. (a) Two-pole case. (b) Four-pole case.

Fig. 19. Summed response of adjacent four-pole filters.

Fig. 22. Full boost results for adjacent two-pole filters.

Fig. 20. Phase responses for two-pole and four-pole filters.
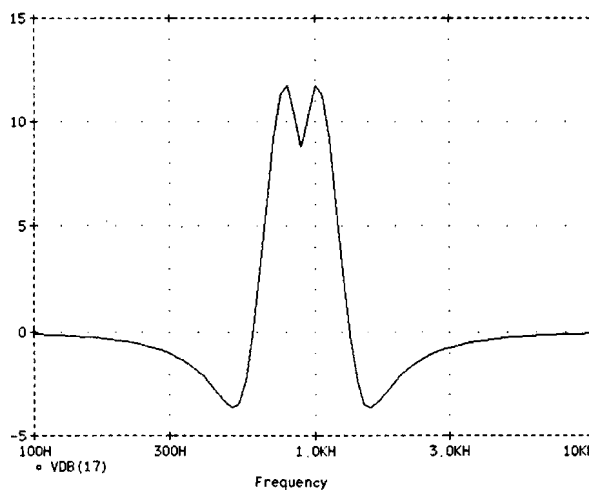

Fig. 23. Full boost results for adjacent four-pole filters.

4.2 Bandpass Filter Topology

Up to this point all discussions concerned a generic bandpass filter. Gone of the elegant aspects of constant-Q topology is the total-isolation of the bandpass filter sections. This allows the bandpass function to be realized in any manner whatsoever. It may be implemented passively or actively, using any topology that realizes a second-order bandpass transfer function. Yes, even gyrators work. It has been said before and it must be said again: it does not matter how a transfer function is realized; two circuits resulting in identical transfer functions will behave *identically*— same phase behavior, same transient behavior. If differences exist, they are due to something other than the topologies used.

Proper selection of the bandpass filter topology involves many trade-offs, not the least of which is cost. For those cost-is-no-object designs, state-variable bandpass circuits [17] are the best choice. (such as, Audioarts 2700). They require three to four operational amplifier per bandpass section, but offer excellent stability and sensitivity. (Sensitivity is a measure of the effect of nonideal components on an otherwise ideal response.)

Next in line, costwise, would be passive and gyrator approaches. Passive bandpass filters involve all the well-known problems of using inductors. In addition, if constant-Q behavior is to be maintained, their outputs require buffering from the loading effects of the slider. Gyrators may be substituted for the inductors; however, at least two operational amplifiers per section will be required.

This brings up the next category of active two-pole RC filters. Requiring only one operational amplifier per section, they represent the most cost-effective approach to constant-Q design. While this category of filters is more sensitive to component tolerances than the state-variable approach, the cost advantages are overwhelming. For significantly less money than the cost of the additional two or three operational amplifiers, some very precise passive components can be bought. With precision parts it has been demonstrated (for ex-
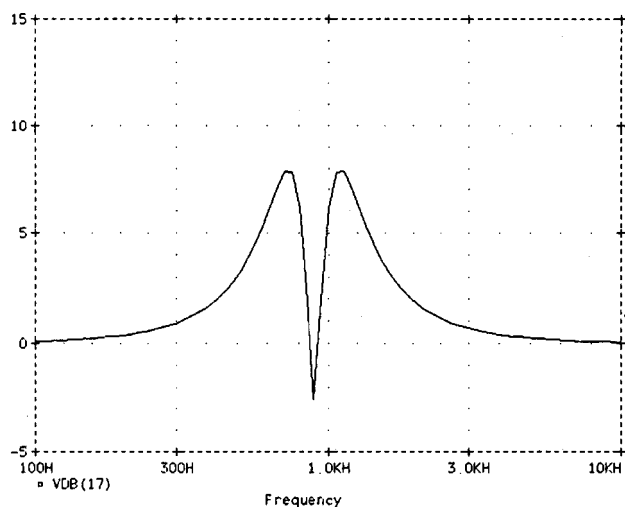
ample, Rane GE 27 and Yamaha GQ1031) that single operational amplifier designs can be mass-produced repeatedly without trim pots.

Selection from among the various configurations of active RC two-pole bandpass filters is no easy task. Two circuits, however, emerge as time-tested and worthy of further study. Both have been derived from the monumental work of Sallen and Key [18].

The first is the well-known voltage-controlled voltage source (VCVS) bandpass filter credited to Kerwin and Huelsman [19], and shown in Fig. 25. It is the most popular *noninverting* configuration and features a low spread of element values. A definite advantage is the ability to precisely set the gain of the filter with resistors R_4 and R_5, without upsetting the center frequency. This circuit drops right into the BP block shown in Fig. 14 since it must be noninverting for the summing to be correct.

The second circuit, shown in Fig. 26, is the equally well-known infinite-gain multiple feedback (MFB) bandpass filter, also credited to Huelsman [20]. This is the most popular *inverting* configuration. It features two fewer resistors-than the VCVS circuit and has excellent stability characteristics due to its lower sensitivities. To apply the MFB configuration to Fig. 14 requires that an inverter be put in series with the inputs leading to all of the filters. One inverter driving all inputs in parallel is sufficient.

Both of these circuits work well in constant-Q graphics and are being used in production today by at least two manufacturers.

4.3 Perfecting the Summing Response

"Combining" is another badly abused term in the professional audio community. The debate goes on regarding combining filters versus noncombining filters, Point of clarification: there is no such thing as a combining *filter.*

The outputs of filter banks combine (or actually,

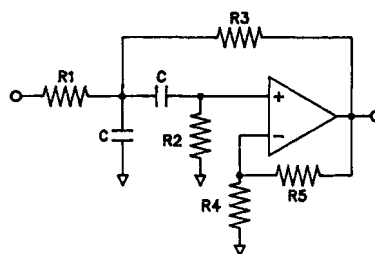Fig. 24. Same as Fig. 23 except main signal inverted.
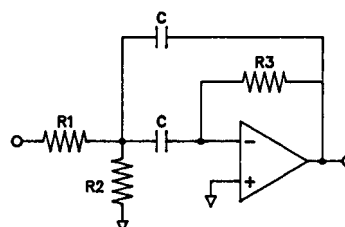

Fig. 25. VCVS bandpass filter.

Fig. 26. MFB bandpass filter.

recombine) to form a resultant curve characterized by a ripple content with associated phase shift. How this combining takes place will dictate how much of each is present. *The type of filter used has nothing to do with it.* Combining is done by electronically summing together all of the filter outputs. It is not a filter at all, it is a summer. All equalizers combine their filter outputs. It is wrong to say an equalizer is noncombining. The only examples of noncombining filters are spectrum and real-time analyzers.

The real issue behind these phrases is how much ripple and phase shift is present in the combined output. This is a fair question, which deserves fair treatment. Fair treatment, however, is not accomplished by apple and orange comparisons. Too often comparisons between constant-Q and conventional graphic equalizers are based on the amount of ripple occurring when two adjacent sliders are boosted a few decibels. Sounds fair, doesn't it? No way—apples and oranges.

What is not examined is the resultant bandwidth from boosting these two adjacent sliders. Doing so would reveal that the constant-Q design produces a resultant curve two-thirds of an octave wide, as it should; and that the conventional design yields a curve over 1.2 octaves wide, which it should not. If the conventional equalizer is set to have the same bandwidth as the constant-Q design, then the combined result will be exactly the same—same transfer function, same result.

There is no doubt that if two adjacent filters located one-third octave apart degrade to where each is one octave wide, the summer result will be very smooth. Fig. 27 illustrates just such a case. By allowing each filter to be one octave wide, the crossover point is only 0.5 dB down. Is it any wonder that they combine smoothly? Compare the results with Fig. 18 and note the extreme bandwidth and magnitude differences. (If the reader feels this to be a contrived or exaggerated example, then please take the nearest conventional equalizer and run a few tests. The results will be very eye-opening.)

The point is that comparisons cannot be made between what are essentially one-octave equalizers (disguised as one-third-octave units) and true one-third-octave graphic equalizers as characterized by constant bandwidth behavior. This does not, however, mean that the combining characteristics of constant-Q designs cannot be improved while still maintaining their narrow bandwidths.

4.4 Two Series Boost/Cut Circuits

A technique used almost universally to improve the combined responses of graphic equalizers involves two series summing circuits. Each is assigned every other one-third-octave filter output for summing. This way two adjacent bands are not added together by the same summer, and the results produce less ripple. This is a valid concept and should work equally well with constant-Q designs.

Fig. 28 shows what this would look like when applied

to the case 1 example. It is drawn simplified, showing the full boost configuration for ease of analysis. As a first point of comparison, two adjacent bands are summed in their full boost positions. The results appear in Fig. 29: quite a difference when compared with Fig. 22—the same case except using only one boost/cut summer. The ripple across the top of the combined result is merely 0.03 dB.

The only negative thing is the increased magnitude. The combined result in Fig. 22 maintains its height quite well but has over 1 dB of ripple, while Fig. 29 shows a combined amplitude of 18.6 dB and essentially no ripple. This increase in magnitude can be predicted from Fig. 28. What is happening is that the input to the second bank of filters has already been made larger by the combined output of the first bank. The "skirt pieces" from adjacent bands become additional input and serve to make the overall output much larger than for the single-summer case.

4.5 Two Nested Boost/Cut Circuits

The circuit in Fig. 30 was developed as a possible solution to this problem. The rationale was to guarantee that all filters have the same input as that in Fig. 14, yet are summed alternately in series, as in Fig. 28.

Again, Fig. 30 is drawn simplified for the full boost configuration. The second boost/cut summing network is now nested between the first boost/cut summing pair. Every other one-third-octave bandpass filter must be inverting (25 Hz, 40 Hz, etc.) for the summing to come out right.

Computer simulation was done on this network with mixed results. The resultant amplitude was less but the ripple was greater. It was felt that the improvement was not significantly better than for the single boost/cut summing circuit.

This circuit is included here for two reasons: 1) to demonstrate that part of why two series summers work so well is due to the "premixing" of the skirt pieces back with the original signal before the result is summed
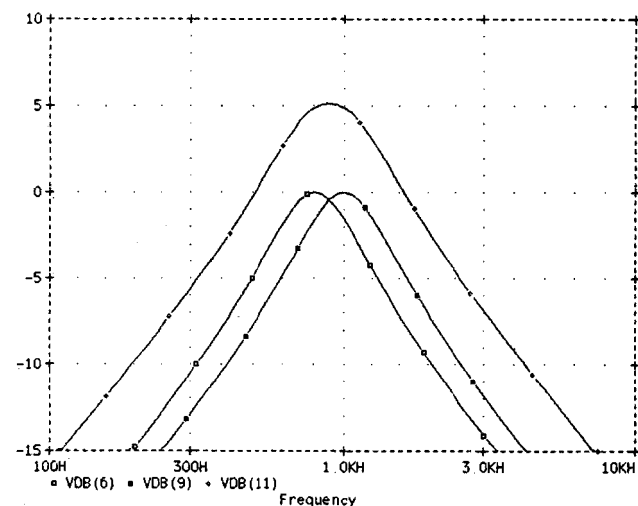

Fig. 27. Summed response of bandwidth degraded adjacent sections.

with the adjacent neighbor, and 2) to stimulate further investigation into alternate ways of combining constant-Q circuitry.

4.6 Optimized Combining Performance

Several important things regarding the optimization of case 1 constant-Q combining characteristics have been learned. A brief summary of these items follows.

1) Design the gain of the bandpass filter sections to be precisely 0 dB at f_0.

2) Design of the exact Q required for the desired bandwidth (for example, one-third-octave bandwidths require a Q of 4.3185). Do not approximate or round off to any other number. The skirts must cross at exactly –3 dB for optimum combining.

3) Design filter center frequencies to be exactly one-
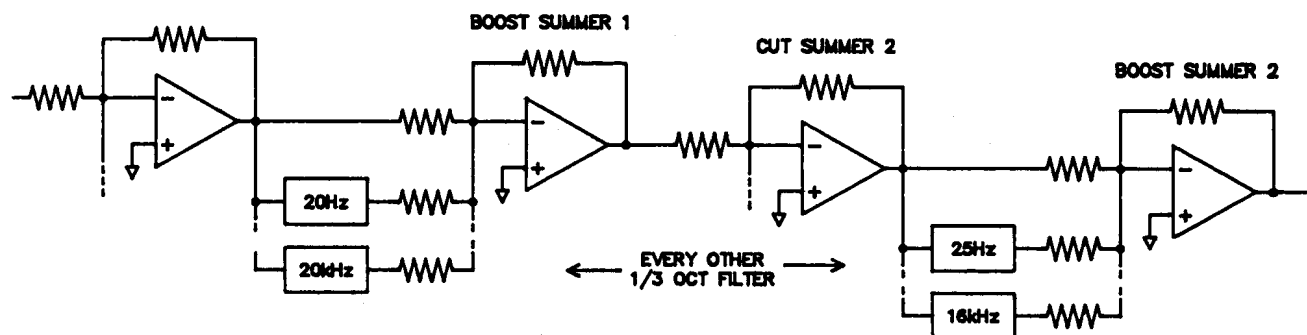

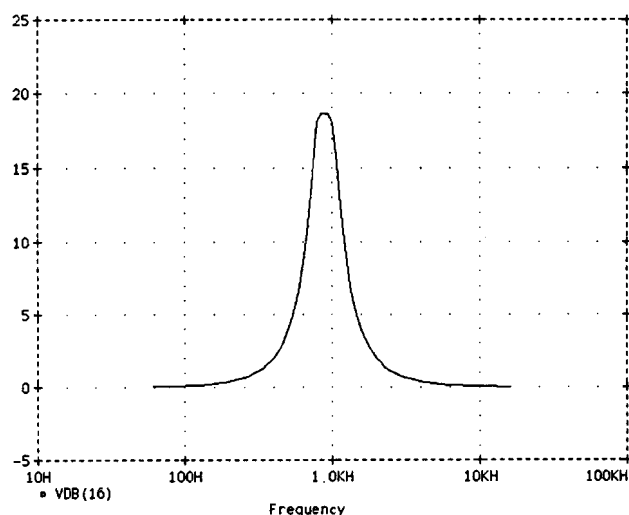Fig. 28. Two series boost/cut circuits.

Fig. 29. Two adjacent bands, full boost, using two summing circuits.

third octave apart. *Do not use the IS0 approximations.* Use 1 kHz as the pivot point and calculate above and below this reference. This means, for example, that the next one-third-octave interval below 1 kHz is 793.7 Hz instead of the IS0 approximation of 800 Hz.

4) Use two series summing networks (three or more do not contribute any better results).

If these seem inordinately picky, they are meant to. Items 2) and 3) alone can make as much as 0.5 dB difference in ripple content. And if the beginning point had only 1 dB to start with, this is a big improvement.

The results of applying the above rules appear in Figs. 31-39. A discussion of each follows.

Fig. 31 shows the results of boosting two adjacent sliders to their 6 dB position for the two-summing-network circuit of Fig. 28. The minimal ripple and the increased amplitude are evident. The ripple is 0.19 dB and the maximum amplitude is 8.1 dB. Compare this
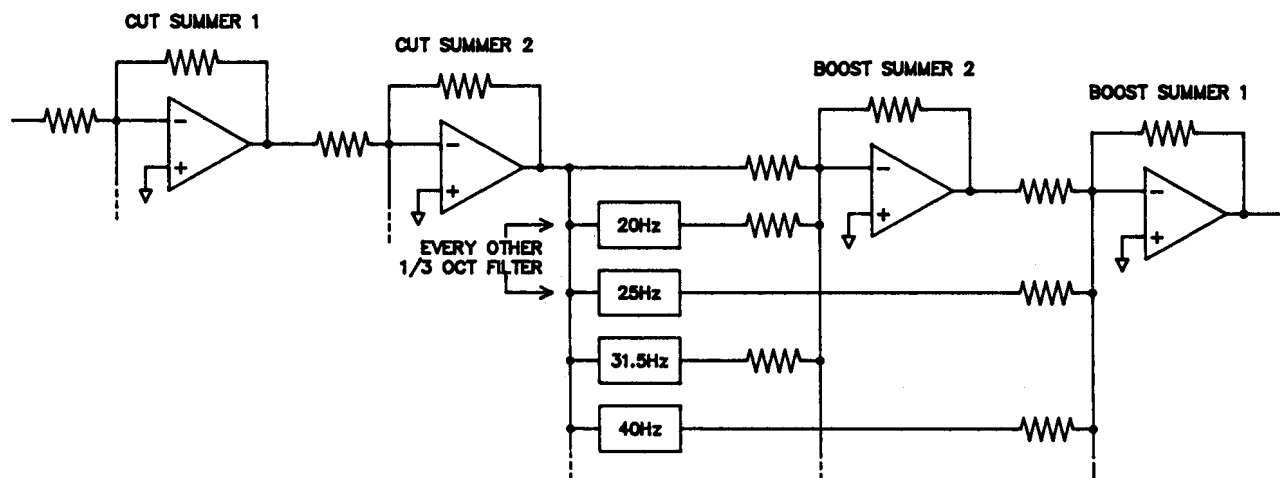

Fig. 30. Common input series boost/cut circuits.

with Fig. 32, where the same conditions appear for the single-summing network of Fig. 14. Here the maximum amplitude is 7 dB, but the ripple is 1 dB. The trade-off is clear.
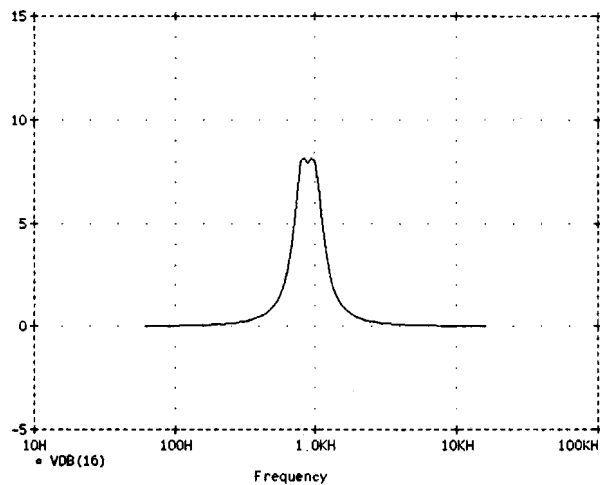
Since the gain of each slider in Fig. 28 can be reduced to match whatever gain is required, this is the preferred choice. Fig. 33 illustrates such an example, where the gain used in Fig. 31 has beep reduced to produce a 6-

Fig. 31. Two adjacent sliders boosted 6 dB; two summing networks.
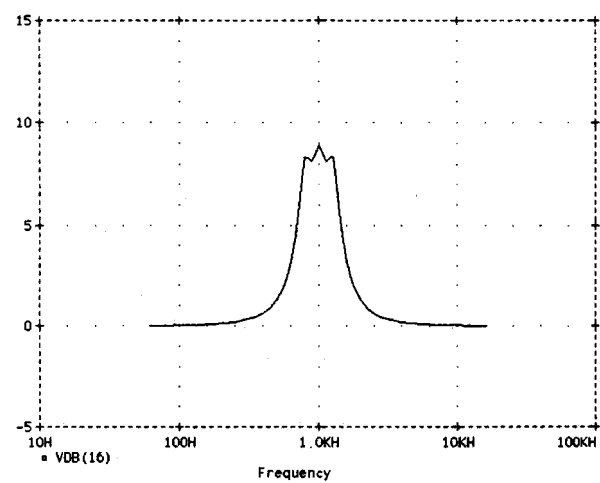

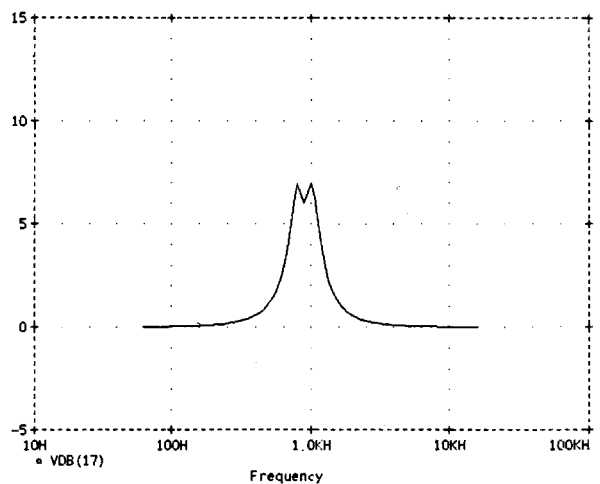Fig. 34. Three adjacent sliders boosted 6 dB, two summing networks.

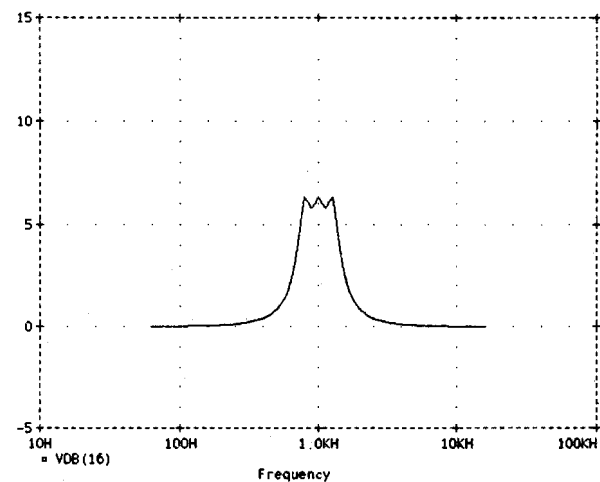Fig. 32 Two adjacent sliders boosted +6 dB, one summing network.

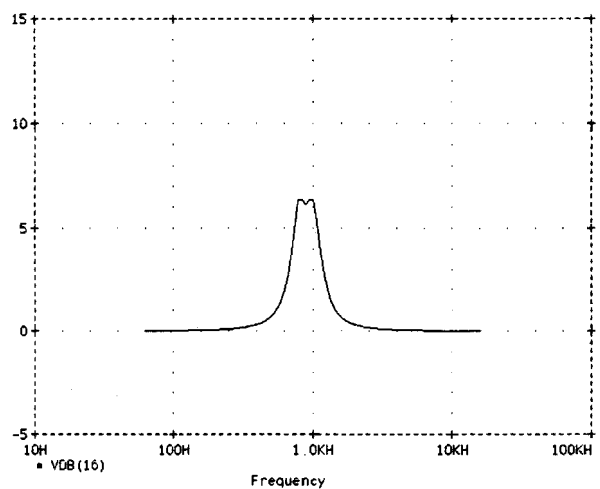Fig. 35. As in Fig. 34, except gain adjusted.

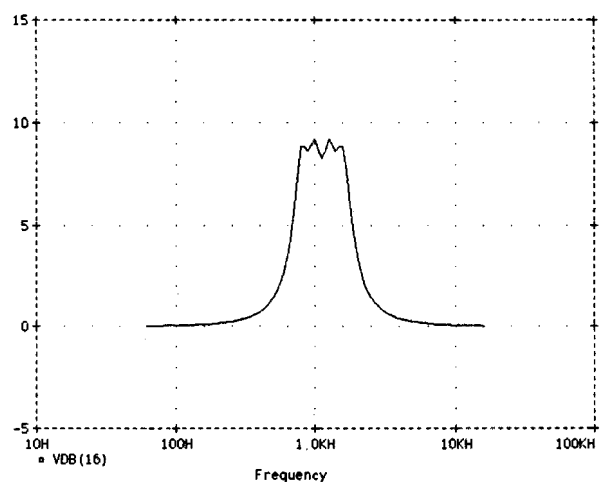Fig. 33. As in Fig. 31, except gain adjusted.

Fig. 36. Four adjacent sliders boosted 6 dB, two summing networks.

dB result. Now compare Figs. 32 and 33.

Fig. 34 shows the result of boosting three adjacent sliders 6 dB. The ripple is 0.8 dB and the maximum amplitude is 8.9 dB. Note that the amplitude did not increase appreciably from that of the two-neighbor case. Fig. 35 shows the gain-adjusted case; now the ripple is only 0.56 dB.

Fig. 36 shows the case of four adjacent sliders for 6 dB of boost. The ripple is 0.57 dB and the maximum amplitude is 9.2 dB. Fig. 37 gives the results of four adjacent bands boosted 12 dB. The ripple is 1.8 dB and the maximum amplitude is 20 dB. Obviously, 20 dB is excessive, but 1.8 dB ripple for full boost is quite good. Most conventional graphics result in the same 20 dB amplitude with 4 dB of ripple, so by comparison these results look good. Incidentally, this is the only condition where constant-Q graphics can be compared fairly with conventional ones regarding combining, since this is the only situation where conventional graphics display one-third-octave bandwidths.

The last two plots show the results of boosting two *alternate* sliders while leaving the adjacent slider centered. Fig. 38 shows the 6 dB case, and Fig. 39 shows the 12 dB case. The two boosted bands reach 6.2 and 12.5 dB, respectively, yielding excellent agreement with the slider settings. The middle sections were suppressed 3.2 and 5.6 dB, respectively. It would be nice to see this deeper, but it is still farbetter than conventional equalizer results [see Fig. 4(b) as a reminder].

4.7 Noise Performance

The case 1 circuit shown in Fig. 8 has a subtle but important noise mechanism that needs to be understood thoroughly if quiet constant-Q designs are to be realized. This noise source involves the noise gain of the summing stages and its relationship to the slider resistance.

Consider the case where all sliders are in their center-detent positions. This ensures that all noise due to the filter sections is grounded and not contributing to the output noise. Now mentally remove the BP filter section, leaving only the paralleled sliders. The remainder can

be redrawn as shown in Fig. 40.

The resistors drawn from the summing nodes to ground represent the equivalent value of the paralleled sliders. Let R_S represent the total resistance of the slider. Since the center is grounded, $R_S/2$ represents the amount of resistance from each summing node to ground. This value divided by n, where n equals the number of sliders, is the equivalent value. As an example, for 30 100k ohm sliders, this value equals approximately 1.7k ohm.

The noise gain of each summing stage is now the feedback resistor R divided by the parallel combination of the input resistor R and the equivalent slider resistance. This is a long way from unity, as a casual observation of this circuit might suggest. Back to the example, if R equaled 100k ohm, the noise gain of each stage would equal 59.8, or 35.5 dB. A choice of 100k ohm is probably not wise.

Unfortunately it is not as easy as just making R smaller. Several factors must be considered and optimized together. The feedback resistor, working against the output resistor of each filter section, determines the maximum amount of boost and cut. In turn, the filter output resistor works against the slider resistance
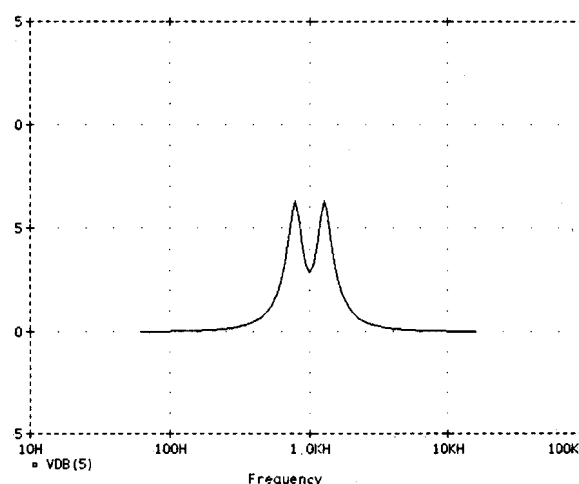

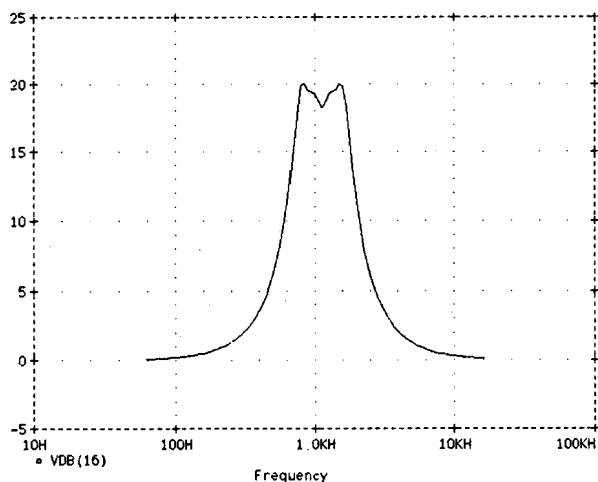Fig. 38. Two alternate sliders boosted 6 dB.

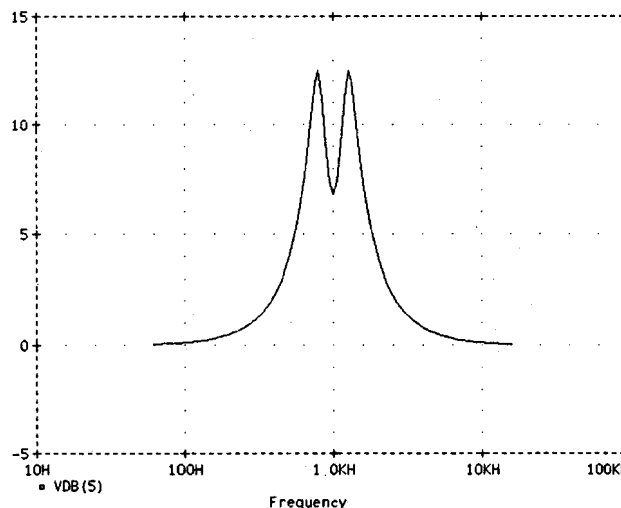Fig. 37. As in Fig. 36, with sliders boosted 12 dB.

Fig. 39. As in Fig. 38, except boosted 12 dB.

(and the feedback resistor), setting the amount of boost and cut for every slider position. A desire for equal linear decibel front panel settings makes this last requirement a little sticky. To make things more interesting, sliders only come in so many values and tapers, none of which, of course, are the ones wanted.

Things are not as difficult as they may appear. It turns out that this circuit tolerates relatively high noise gains while still yielding excellent noise performance. Signal-to-noise ratios exceeding 90 dB have been achieved by several commercial equalizers using this topology.

5 FUTURE RESEARCH

Constant-Q one-third-octave graphic equalizers have evolved into second-generation models. Future research will result in even better units.

Several areas warrant further study. Among these should be ways of improving circuits for the reconstruction of individual filter outputs. The quest for perfect combining continues. Desired is an absolutely smooth net curve whose amplitude agrees absolutely with the front panel controls.

Adjacent band interference needs further minimizing so that the *alternate* slider test yields 0 dB between boosted (or cut) sections. This suggests additional study into ways of using higher order bandpass filters.

Analog and digital transversal filter technology offers the best potential for dramatic advances in future generations of constant-Q graphic equalizers. Much work remains to be done, however, in the areas of circuit applications and cost reduction before transversal filter technology will achieve parity with today's best active RC filter designs.

Little imagination is required to envision the design of a custom-combined analog and digital VLSI chip that is application specific for constant-Q graphic equalizers. All filters on one chip using switched-capacitor filter technology, combined with all necessary clock-generating circuitry, is the stuff of sweet dreams. Using very narrow silicon-gate CMOS technology, such a chip can be designed today. With one exception, the drawback is not technology, it is cost.

The exception is the need for a higher voltage CMOS process. Headroom requirements dictate the use of larger supply voltages than are possible today; however, there are ways around this problem. There are fewer ways around the price. Development costs for VLSI chips are very steep. By itself, this might be justified if the market were big enough to warrant large runs. Full custom VLSI requires a commitment to at least 50,000

chips a year. The market for graphic equalizers is simply not this big.

Development of standard-cell semicustom chips that can be designed to be customer-specific graphic equalizers is a possibility. This would drop both development costs and requirement sizes dramatically. Only time will tell if sufficient markets open up to warrant development of this type of chip.

Enough standard products exist today using. switched-capacitor filter technology [21] to allow the bandpass functions to be implemented. The extra complexity of the clock generating circuits, however, coupled with performance limitations and increased costs, makes their use questionable.

6 SUMMARY

The category of graphic equalizers classified as being constant-Q has been presented and shown to offer significant advantages over conventional RLC and gyrator designs.

Various topologies for constant-Q designs have been shown and trade-offs discussed. The case 1 configuration emerged as the best overall approach. Optimization of this example was discussed, where it was demonstrated that second-order filters and two series boost/cut networks offer the best performance. Finally, directions for future research were outlined with the hope that further development of this exciting category will continue.

No doubt, many improvements will appear in the future, but at least it can now be said that constant-Q equalizers are in head-on competition with conventional equalizers— and winning with every evaluation made.

7 REFERENCES

[l] D. Bohn, Ed., *Audio Handbook* (National Semiconductor Corp., 1976), pp. 2-53–2-55.

[2] R. A. Greiner and M. Schoessow, "Design Aspects of Graphic Equalizers," presented at the 69th Convention of the Audio Engineering Society, *J. Audio Eng. Soc. (Abstracts),* vol. 29, p. 556 (1981 July/Aug.), preprint 1767.

[3] D. Bohn, "State-Variable Graphic Equalizers," Rane Corp., Note 101 (1982).

[4] G. Snow, "Model 2700 One-Third Octave Equalizer," Audioarts Engineering Div., Wheatstone Corp., private communication (1985).

[5] D. Nova, "Model EVT 2230 Tapco Graphic Equalizer," Electra-Voice, Gulton Industries, private communication (1985). (Mr. Nova is now with Physio-Control Corp., Redmond, WA.)

[6] R. Riordan, "Simulated Inductors Using Differential Amplifiers," *Electron. Lett.,* vol. 3, pp. 50-51 (1967 Feb.).

[7] T. Pennington, "Constant Q," *Studio Sound,* vol. 27, pp. 82-85 (1985 Oct.).

[8] T. H. Ishimoto, "Application of Gyrators in Graphic Equalizers," presented at the 63rd Convention of the Audio Engineering Society, *J. Audio Eng. Soc. (Abstracts),* vol. 27, p. 598 (1979 July/Aug.), preprint 1501.
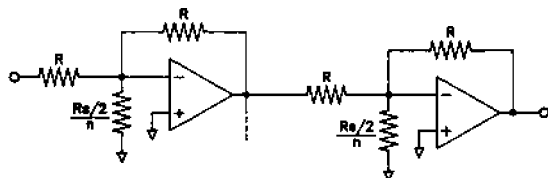
Fig. 40. Equivalent circuit for noise analysis.

[9] D. Bohn, "A New Generation of Filters," *Sound and Video Contractor,* vol. 2, pp. 36-39 (1984 Feb. 15).

[10] T. Pennington, "The Facts As They Pertain to l/3-octave Equalizer Performance," Rane Corp. (1985).

[11] K. Gundry, U.K. Patent 1,452,920 (1973 Nov.).

[12] C. Van Ryswyk, "Filters for Equalization: Active or Passive?" presented at the 55th Convention of the Audio Engineering Society, *J. Audio Eng. Soc. (Abstracts),* vol. 24, p. 851 (1976 Dec.), preprint 1177.

[13] C. Van Ryswyk, "Sound Reinforcement Equalization System," U.S. Patent 3,755,749 (1973 Aug. 28).

[141 "Transversal Equalizer DG-4017," Industrial Research Products, Inc., data sheet (1984).

[15] H. Blinchikoff and A. Zverev, *Filtering in the Time and Frequency Domains* (Wiley, New York, 1976).

[16] D. Bohn, "Bandpass Filter Design," *Studio Sound,* vol. 25, pp. 36-37 (1983 Jan.).

[17] W. Kerwin, L. Huelsman, and R. Newcomb, "State-Variable Synthesis for Insensitive Integrated Circuit Transfer Functions," *IEEE J. Solid-State Circuits,* vol. SC-2, pp. 87-92 (1967 Sept.).

[18] R. Sallen and E. Key, "A Practical Method of Designing RC Active Filters," *IRE Trans. Circuit Theory,* vol. CT-2, pp. 74-85 (1955 Mar.).

[19] W. Kerwin and L. Huelsman, "The Design of High Performance Active RC Bandpass Filters," *IEEE Int. Conv. Rec.,* vol. 14, pt. 10 (1960), pp. 74-80.

[20] L. Huelsman, *Theory and Design of Active RC Circuits* (McGraw-Hill, New York, 1968).

[21] K. Lacanette, Ed., *The Switched-Capacitor Filter Handbook* (National Semiconductor Corp., 1985).

THE AUTHOR

Dennis A. Bohn was born in San Fernando, California, in 1942. He received B.S.E.E. and M.S.E.E. degrees from the University of California at Berkeley in 1972 and 1974, respectively. Between undergraduate and graduate schools, he worked as a research and development engineer for the Hewlett-Packard Company developing thin-film high-speed oscillators. Upon completion of his M.S.E.E., he accepted a position with National Semiconductor Corporation as a linear application engineer specializing in audio. While at National Semiconductor, he created the *Audio Handbook,* acting as technical editor and contributing author. In 1976, he accepted the position of senior design engineer for Phase Linear Corporation, where he was involved in designing several consumer audio products. Promoted to engineering manager in 1978, he was responsible for developing the professional audio products division.

In 1982 Mr. Bohn's strong interest in professional audio products prompted him to leave Phase Linear and accept the position of vice president of engineering for Rane Corporation. In 1984, Dennis became a principal of Rane Corporation and assumed the position of vice president in charge of research and development, where he now designs and develops advanced analog and digital products for the professional audio industry.

Mr. Bohn is a member of the AES, the IEEE, and Tau Beta Pi. For the past two years he has been listed in Who's Who **in** the West. Dozens of articles written by him have appeared in national and international magazines. He has also presented many papers at conventions of the Audio Engineering Society.